Title: A Metabolomic Signature of Acute Caloric Restriction.

Authors: Collet TH, Sonoyama T, Henning E, Keogh JM, Ingram B, Kelway S, Guo L, Farooqi IS

Journal: The Journal of clinical endocrinology and metabolism

Year: 2017 Sep 28

DOI: 10.1210/jc.2017-01020

A Metabolomic Signature of Acute Caloric Restriction

Tinh-Hai Collet M.D., Takuhiro Sonoyama M.D. PhD., Elana Henning B.Soc.Sc., Julia M. Keogh BSc., Brian Ingram PhD., Sarah Kelway BSc., Lining Guo PhD., I. Sadaf Farooqi M.D. PhD

The Journal of Clinical Endocrinology & Metabolism
Endocrine Society

Submitted: May 02, 2017
Accepted: September 19, 2017
First Online: September 28, 2017

The Journal of Clinical Endocrinology & Metabolism; Copyright 2017 DOI: 10.1210/jc.2017-01020

A Metabolomic Signature of Acute Caloric Restriction

Tinh-Hai Collet M.D., Takuhiro Sonoyama M.D. PhD., Elana Henning B.Soc.Sc., Julia M. Keogh BSc., Brian Ingram PhD., Sarah Kelway BSc., Lining Guo PhD., I. Sadaf Farooqi M.D. PhD.

From the University of Cambridge Metabolic Research Laboratories and NIHR Cambridge Biomedical Research Centre (T.H.C., T.S., E.H., J.M.K., S.K., I.S.F.), Wellcome Trust-MRC Institute of Metabolic Science, Addenbrooke's Hospital, Cambridge, CB2 0QQ, UK; Service of Endocrinology, Diabetes and Metabolism (T.H.C.), University Hospital of Lausanne, 1011 Lausanne, Switzerland; Metabolon Inc. (B.I., L.G.), 617 Davis Drive, Suite 400, Durham, NC 27713, USA.

Received 02 May 2017. Accepted 19 September 2017.

Context:
The experimental paradigm of acute caloric restriction followed by refeeding can be used to study the homeostatic mechanisms that regulate energy homeostasis, which are relevant to understanding the adaptive response to weight loss.
Objective:
Metabolomics, the measurement of hundreds of small molecule metabolites, their precursors, derivatives, and degradation products, has emerged as a useful tool for the study of physiology and disease and was used here to study the metabolic response to acute caloric restriction.
Participants, Design and Setting:
We used four ultra high performance liquid chromatography-tandem mass spectrometry methods to characterize changes in carbohydrates, lipids, amino acids and steroids in eight normal weight men at baseline, after 48 hours of caloric restriction (CR; 10% of energy requirements) and after 48 hours of *ad libitum* refeeding in a tightly-controlled environment.
Results:
We identified a distinct metabolomic signature associated with acute CR characterized by the expected switch from carbohydrate to fat utilization with increased lipolysis and beta-fatty acid oxidation. We found an increase in omega-fatty acid oxidation and levels of endocannabinoids which are known to promote food intake. These changes were reversed with refeeding. Several plasmalogen phosphatidylethanolamines (endogenous anti-oxidants) significantly decreased with CR (all $p \leq 0.0007$). Additionally, acute CR was associated with an increase in the branched chain amino acids (all $p \leq 1.4 \times 10^{-7}$) and dehydroepiandrosterone sulfate ($p=0.0006$).
Conclusions:
We identified a distinct metabolomic signature associated with acute CR. Further studies are needed to characterise the mechanisms that mediate these changes and their potential contribution to the adaptive response to dietary restriction.

We conducted a metabolomic analysis of 770 small molecules in eight healthy lean men and identified a distinct metabolomic signature associated with acute caloric restriction.

Introduction

The adipocyte-derived hormone leptin circulates at concentrations proportional to fat mass in weight-stable humans and is a pivotal regulator of energy homeostasis [1-3]. Most individuals maintain a relatively stable body weight over long periods of time despite day-to-day fluctuations in the number of calories consumed and the amount of physical activity undertaken.

Loss of fat mass leads to a fall in circulating leptin concentrations triggering changes in energy intake, energy expenditure and neuroendocrine function that restore energy homeostasis, resulting in rebound weight gain - the phenomenon popularly known as yo-yo dieting. Rosenbaum and Leibel have shown that leptin administration in short-term human studies can reverse many of the consequences of weight loss (a state of partial leptin deficiency) [4, 5]. However, recombinant leptin/leptin mimetics are not currently available for this purpose. The identification of additional markers of the homeostatic response to weight loss could inform therapeutic strategies to prevent weight regain and aid weight maintenance.

In seminal studies in mice, Ahima and Flier showed that as well as being a marker of fat mass, leptin acts as a signal of nutrient availability; acute caloric restriction/starvation (without loss of fat mass), leads to a rapid fall in circulating leptin concentration, hyperphagia, reduced energy expenditure and hypogonadism [6], features which mimic genetic leptin deficiency in rodents and humans [7, 8] and can be normalized by leptin administration [6, 9]. Acute caloric restriction (CR) in humans can therefore be used as a model for investigating leptin-mediated homeostatic responses without the potential confounding effects of weight loss.

The metabolomic profile at a given timepoint represents the cumulative effects of the diet, genome, transcriptome, proteome and gut microbiome–host interaction on small molecule metabolites whose concentrations change rapidly [10]. By measuring the metabolome in the same individuals before and after a precise perturbation, our aim was to identify the metabolites which change significantly with acute CR and refeeding. We assessed the short-term adaptation to CR to avoid confounding with metabolic changes related to weight loss.

We performed a carefully-controlled experimental study to directly examine the effects of acute CR in eight normal weight young men housed in a Clinical Research Facility where diet, fluid intake, timing of meals and sleep were precisely controlled and monitored (**Supplementary Table 1**). Fasting blood samples were obtained at three timepoints: baseline (after 24hr feeding to normal energy requirements); after 48 hours of CR to 10% of their normal energy requirements (mean 226 ± SEM 5 kcal/day); after 48 hours of *ad libitum* refeeding (RF) to allow for energy homeostasis to be reset. Critically, the proportion of macronutrients received during CR was the same as on the baseline day (50% carbohydrate, 30% fat, 20% protein). In a previous study, we have shown that this experimental manipulation is sufficient to significantly alter physiological parameters including autonomic function, neuroendocrine hormone secretion and the sleep/wake cycle [11]. Here, in addition to measuring circulating hormones and peptides predicted to be altered by nutritional status (e.g. leptin, insulin, glucagon, thyroid hormones), we used a high throughput metabolomics assay employing four independent ultra high performance liquid chromatography-tandem mass spectrometry (UPLC-MS/MS) methods to measure 770 small molecule metabolites involved in carbohydrate, fat, protein and steroid metabolism.

Material and Methods

Experimental design of study

The study was approved by the Cambridge local research ethics committee and was conducted in accordance with the principles of the Declaration of Helsinki. Written informed consent was received from each participant prior to inclusion in the study. We recruited eight normal weight healthy men using the following inclusion criteria: normal glucose tolerance measured by a 75-gram oral glucose tolerance test, no evidence of renal, liver or thyroid disease, average alcohol intake <2 units/day, not participating in an organized exercise program, not treated with anorectic agents or medications known to affect carbohydrate and/or lipid metabolism, or blood pressure. Shift workers were excluded from the study; all participants had a normal sleep/wake pattern as determined by polysomnography at screening. Weight and height were measured barefoot in light clothing and body mass index calculated (weight in kg/height in meters squared). Baseline characteristics are provided in **Supplementary Table 1**.

Participants were resident on the NIHR-Wellcome Trust Clinical Research Facility, Addenbrooke's Hospital, Cambridge, UK, for the duration of the study under direct observation throughout. At baseline, volunteers consumed a balanced diet (50% carbohydrate, 30% fat, 20% protein) matching their daily energy requirement calculated by the basal metabolic rate multiplied by a physical activity level of 1.25 using the Schofield equation [12]. To manipulate energy balance, baseline measurements were followed by CR to 10% of normal energy requirement (mean 226 ± SEM 5 kcal/day) for two days. After CR, participants were offered three substantial *ad libitum* buffet meals per day (20 MJ = 4777 kcal) and additional snacks (16 MJ = 3821 kcal) between meals for two days. They were invited to eat freely until comfortably full; food consumption was covertly measured. Fluid intake was fixed for all participants; no coffee/tea/alcohol was permitted. All meals were given at the same time each day. Timing of "lights out" and waking were controlled. We collected fasting serum and plasma samples at 0800 a.m. at baseline, after CR, and RF.

Biochemical assays

Plasma glucose, insulin, glucagon, leptin, serum lipids, thyrotropin, free thyroxine (T4), and free tri-iodothyronine (T3). Testosterone and dehydroepiandrosterone sulfate (DHEAS) were measured with a DiaSorin Liaison XL analyzer (Saluggia, Italy), and 3-hydroxybutyrate using the Stanbio colorimetric kit (Boerne, TX). Blood samples were collected in the fasting state at 08:00 a.m.

Metabolomic platform

The non-targeted metabolomic analysis was performed at Metabolon, Inc. (Durham, North Carolina, USA). All serum samples were stored at –80°C until processed. The detailed descriptions of the platform, including sample processing, instrument configuration, data acquisition, and metabolite identification and quantitation, were published previously [10] with the exception that four independent UPLC-MS/MS methods were used. The samples were extracted with methanol and the supernatants were divided into five equal fractions for analysis by UPLC-MS/MS: 1) reverse phase (RP) UPLC-MS/MS method with positive ion mode electrospray ionization (ESI), optimized for more hydrophilic compounds. In this method, the extract was gradient eluted from a C18 column (Waters UPLC BEH C18-2.1x100 mm, 1.7 µm) using water and methanol, containing 0.05% perfluoropentanoic acid (PFPA) and 0.1% formic acid (FA); 2) RP/UPLC-MS/MS method with positive ion mode ESI, optimized for more hydrophobic compounds. In this method, the extract was gradient eluted from the same afore mentioned C18 column using methanol, acetonitrile, water, 0.05% PFPA and 0.01% FA and was operated at an overall higher organic content; 3) RP/UPLC-MS/MS method with negative ion mode ESI. In this method, the extract was gradient eluted from the column using methanol and water, however with 6.5mM Ammonium Bicarbonate at pH 8; 4) hydrophilic interaction liquid chromatography (HILIC)/UPLC-MS/MS with negative ion mode ESI. In this method, the extract was gradient eluted using water and acetonitrile with 10 mM ammonium formate, pH 10.8; and 5) reserved for backup. For UPLC-MS/MS, all methods utilized a Waters ACQUITY ultra-performance liquid chromatography (UPLC) and a Thermo Scientific Q-Exactive high resolution/accurate mass spectrometer interfaced with a heated electrospray ionization (HESI-II) source and Orbitrap mass analyzer operated at 35,000 mass resolution. All the methods alternated between full scan MS and data-dependent MS^n scans using dynamic exclusion. The scan range varied slighted between methods but generally covered 70-1000 m/z.

The structure of metabolites were identified by automated comparison of the ion features in the experimental samples to a reference library of chemical standard entries that included retention time, molecular weight (m/z), preferred adducts, and in-source fragments as well as associated MS spectra and curated by visual inspection for quality control using software developed at Metabolon [13-15].

Statistical analyses

Statistical analyses of biochemistry results.
Log-transformed values were analyzed using analysis of variance (ANOVA) with repeated measures to test for within-subject changes across the three study conditions (baseline, CR, refeeding). The within-subjects p-value was adjusted using the Greenhouse-Geisser correction factor for lack of sphericity. Pairwise comparisons of the three study conditions were performed by two-sided Student's t-test when appropriate. A p-value of 0.05 was considered significant after Bonferroni correction for multiple comparisons.

Statistical analyses of metabolite semi-quantitative levels.
Following scaling of the ion count (so that the median equals 1), imputation of any missing values with the minimum observed value for each metabolite and log transformation, ANOVA contrasts and Welch's matched-pair t-tests were used to identify biochemicals that differed significantly between experimental groups. Multiple comparisons were accounted for with the false discovery (FDR) rate method [16]. An estimate of the false discovery rate (q-value) was calculated to take into account the multiple comparisons that normally occur in metabolomic-based studies. A low q-value ($q<0.10$) is an indication of high confidence in a result. While a higher q-value indicates diminished confidence, it does not necessarily rule out the significance of a result. Principal components analysis (PCA) and hierarchical clustering of scaled, imputed and log-transformed metabolite levels are detailed in the Supplementary Methods. Statistical analyses were performed using JMP (SAS, http://www.jmp.com) and R software (http://cran.r-project.org/).

Results

A Metabolomic Signature of Caloric Restriction
Acute CR was associated with a significant fall in circulating fasting leptin, insulin and glucose concentrations and an increase in glucagon levels (**Table 1**). We noted a decrease in free T3 but no significant change in thyrotropin or free T4 in response to acute CR as seen in some previous studies [17, 18]. Most parameters returned to baseline values with refeeding whilst others (insulin, glucagon) were sensitive to the overconsumption of calories on *ad libitum* refeeding and exceeded baseline values (**Table 1**).

We explored the metabolomic profile for each participant at baseline, CR and in the refed state by employing multivariate statistical analyses to analyse state-dependent changes. PCA was conducted on log-transformed metabolite levels to identify whether aggregated values of specific components could account for a proportion of the variability between baseline, CR and refeeding. We found that the PCA of the metabolome completely distinguished the three states revealing a characteristic metabolomic signature associated with CR (**Figure 1A**). Whilst within a state, there was variability between participants (presumably due to genetic/biological factors), the magnitude and direction of effect of CR and refeeding was comparable for all participants (**Supplementary Figure 1**).

A substantial proportion of the entire metabolome exhibited a dynamic response to CR and refeeding (**Figure 1B**). We used hierarchical clustering to identify large-scale differences in metabolite categories for each individual in each state. The resulting heatmap revealed that CR induced a number of changes in lipid and carbohydrate utilization; some of which were reversed upon refeeding (**Figure 1C**). Further discussion is focused on metabolites that constitute this dynamic metabolomic signature. The complete dataset is presented in **Supplementary Table 2** an associated interactive webpage is available (link active on publication).

Carbohydrate utilization: glycolysis and the TCA cycle

Classically, glycolysis converts glucose to pyruvate, which, under aerobic conditions, is converted into acetyl-CoA, the entry point into the tricarboxylic acid (TCA) cycle (**Figure 2A**). As expected, CR was associated with a decrease in glucose (fold change 0.84, $p=5.9 \times 10^{-5}$) and pyruvate (fold change 0.32, $p=9.0 \times 10^{-4}$) which were restored by refeeding (fold change 1.14 and 10.8, $p=8.0 \times 10^{-4}$ and 1.2×10^{-7}, respectively) (**Figure 2A**). Citrate and aconitate were significantly elevated with CR, there was no change in isocitrate or alpha-ketoglutarate, but a significant decrease in succinylcarnitine, an intermediate arising reversibly from succinyl-CoA (**Figure 2A**). N-acetyl derivatives of the glucogenic amino acids glycine, serine and alanine increased with CR and decreased with refeeding (**Figure 2B**). In contrast, glutamate and its product N-acetylglutamate decreased with CR (**Figure 2B**). These changes reversed upon refeeding and collectively are consistent with an increase in metabolite flux through the TCA cycle in response to CR.

While some N-acetylated amino acid derivatives followed the same pattern across baseline-CR-RF conditions as their corresponding amino acids (e.g. Glutamate, Serine), others did not (e.g. Glycine, Alanine, Figure 2B). The reasons for the differential effects of CR on N-acetylation of gluconeogenic amino acids need further investigation.

Lipolysis and Fatty acid oxidation

CR was characterized by lipolysis of triglycerides generating increased levels of glycerol (2.43 fold, $p=0.0003$), decreased monoacylglycerols and an increase of all long and most medium chain fatty acids detected (**Figure 3A-C**). During CR, we found a significant increase in long-chain acylcarnitines which shuttle fatty acids into mitochondria (**Figure 3D**). Consequently, the ketone bodies acetoacetate and 3-hydroxybutyrate, final products of the fatty acid β-oxidation pathway, were markedly increased with CR ($p=1.6 \times 10^{-11}$ and $p=2.0 \times 10^{-11}$, respectively) and decreased with RF ($p=4.9 \times 10^{-13}$ and 1.6×10^{-12}, respectively) (**Figure 3E**). Serum levels of ketone bodies were measured in routine laboratory tests for comparison; 3-hydroxybutyrate increased 17.3 fold (**Table 1**).

Additionally, 3-hydroxy fatty acids were increased in keeping with increased lipolysis and fatty acid β-oxidation (**Figure 3F**). Furthermore, fatty acid dicarboxylates, in particular dodecanedioate and tetradecanedioate, which increased 7.7-fold on CR, are generated through the ω-oxidation pathway (**Figure 3F**). Whilst this pathway has rarely been studied in humans, our study suggests that activation of ω-oxidation may occur when β-oxidation becomes overwhelmed as it may in CR. Taken together, CR resulted in increased reliance on fatty acid (rather than carbohydrate) metabolism to fuel energy production. Refeeding led to a decreased reliance on fatty acid oxidation to meet energetic needs and stimulation of lipogenesis (**Figures 3B-F**).

Phospholipids and endocannabinoids

Whilst triglycerides represent the major source of stored lipid, phospholipids are the major constituents of plasma membrane lipids and eicosanoids such as prostaglandins, leukotrienes and thromboxanes. We found that most glycerophospholipids and their product lysolipids were decreased in CR and increased upon refeeding (**Figure 4A-C**). Plasmalogens are a subclass of glycerophospholipids that serve as endogenous anti-oxidants, protecting membrane lipids and lipoprotein particles from excessive oxidation by scavenging reactive oxygen species via the vinyl ether moiety [19, 20]. Interestingly, the plasmalogen phosphatidylethanolamines (PPEs), but not the plasmalogen phosphatidylcholines (PPCs), decreased on CR and increased with refeeding (**Figure 4B**).

Sphingolipids play a role in the formation of membrane lipid rafts, are components of plasma lipoprotein associated particles and act as ligands for specific cell-surface receptors. In our study, the most abundant sphingolipids, the sphingomyelins, increased with CR; this pattern was reversed in the refed state (**Figure 4D**). Sphingosine, sphingosine-1-phosphate (S1P) and ceramides are interconvertible sphingolipid metabolites; many studies have shown that their relative levels regulate cell fate [21, 22]. Levels of sphingosine (generally associated with growth arrest and cell death) decreased in CR (0.52 fold, p=0.03) whilst there was no change in S1P which is involved in cell growth and survival.

Another group of lipid signaling molecules, the endocannabinoids, modulate energy intake and expenditure by acting on central neural pathways expressing the cannibinoid 1 receptor, a target of the weight-loss agent rimonabant [23]. Whilst there was no change in 2-arachidonoyl glycerol (2-AG), the most abundant endogenous ligand of cannabinoid receptors which has a very short half-life (**Supplementary Table 2**), all other detected endocannabinoids increased in CR then decreased upon refeeding (**Figure 4E**). These findings are consistent with experimental evidence in animals where a key role for endogeneous endocannabinoids is to stimulate food intake [24].

Amino acids and their derivatives

Several amino acids and their metabolites (in particular Tryptophan and its derivatives) decreased in CR, then increased with refeeding (**Figure 1C**; **Supplementary Table 2**); these changes may in part reflect reduced dietary intake. In contrast, the three branched chain amino acids (BCAAs), leucine, isoleucine and valine significantly increased upon CR (all $p \leq 1.4 \times 10^{-7}$, **Figure 5A**). BCAAs are degraded by the branched-chain alpha-keto acid dehydrogenase complex into acyl-CoA derivatives, which are converted into acetyl-CoA or succinyl-CoA that enter the TCA cycle. We observed increased levels of many BCAA catabolites consistent with accelerated BCAA catabolism under CR which reversed upon refeeding (**Supplementary Figure 2**).

Steroid Metabolism

In contrast to cortisol which changes minimally with age, circulating concentrations of the adrenal steroid hormone DHEAS are high during early adulthood then decline markedly with age [25]. Some, but not all, studies in primates and humans [26] have suggested that chronic CR may affect DHEAS levels. In this study, 48 hours of CR was associated with an increase in DHEAS and the steroid hormones pregnenolone and androsterone; values returned to baseline levels on refeeding (**Figure 5B and Supplementary Figure 3**). Cortisol levels did not change significantly during the study (**Supplementary Table 2**).

Discussion

Using an experimental design in which we stabilized dietary intake across participants for 24 hours before an observed period of acute CR, followed by *ad libitum* refeeding to restore energy homeostasis, we identified a characteristic metabolomic signature associated with acute CR. Some of our findings align with previous studies that have measured targeted sets of metabolites in response to an overnight/prolonged fast [27, 28]. Whilst changes in glycolysis and markers of fatty acid β-oxidation were predicted, our study shows that ω-oxidation (generally regarded as a minor fatty acid oxidation pathway in humans) may be activated in response to acute CR in healthy individuals. ω-oxidation is utilized as part of the compensation for defective beta or alpha-fatty acid oxidation in rare genetic disorders such as Refsum's disease and X-linked adrenal leukodystrophy [29].

We saw consistent class-wide changes in several lipid species (phospholipids, sphingolipids and endocannibinoids) which may reflect the mobilisation of fatty acids for energetic purposes. In keeping with this hypothesis, CR/RF induced changes in fatty acids correlated with changes in their respective fatty acyl carnitines (**Supplementary Figure 4**). Additionally, we observed a negative correlation between the change in fatty acid levels and the change in lysophosphatidylcholines with CR (**Supplementary Figure 5**), an effect that may be mediated by NTE neuropathy target esterase)-related esterase, an enzyme which has lysophospholipase activity, is expressed in adipose tissue and skeletal muscle, and is upregulated upon fasting [30].

By focussing on the 27 long chain fatty acids and polyunsaturated fatty acids examined in this study (**Figure 3C**), we observed that palmitoleate (16:1), a major constituent of the glycerides in human adipose tissue that has been associated with increased insulin sensitivity [31], exhibited a highly significant change with CR (3.61-fold, $p=1.9 \times 10^{-5}$). In contrast, arachidonate, a major omega-6 fatty acid and precursor of lipid-derived mediators of inflammation (leukotrienes and thromboxanes) changed least in response to CR (**Figure 3C**). Thus, whilst the whole scale changes in fatty acids we observed during CR represent the activation of fatty acid oxidation to supply energetic needs, specific changes in fatty acids may predispose to increased insulin sensitivity and reduced cellular inflammation, findings which have potential relevance to protection from aging [32, 33] and require further exploration.

In this study, we identified a series of metabolite changes associated with acute CR without weight loss. The changes in carbohydrate, lipid and amino acid metabolism that we observed are characteristic of the counter-regulatory response that acts to defend against starvation and restore energy homeostasis. Whilst this degree of CR is seldom experienced by most people, short-term CR for weight loss engages the same physiological and biochemical mechanisms. The activation of these mechanisms, whose function is to restore energy balance, underpins weight regain, the phenomenon popularly known as yo-yo dieting. The application of metabolomics analyses to carefully controlled studies of weight loss and the comparison with the dataset reported here, may reveal novel biomarkers that predict the degree of weight loss/regain.

Experimental studies in animal models have consistently shown that CR, typically 40-60% of energy requirements, can extend lifespan by up to 50% compared to *ad libitum* fed animals [34-36]. Our study permits comparison with a large body of research into the effects of CR in lower organisms, although there are challenges in comparing data across species and from serum rather than cells/tissues [37, 38]. One particularly interesting convergence is the finding that some phosphatidylethanolamines (PEs), lipids that are known to affect cell survival and the lifespan of yeast and flies [39], decreased with CR and increased with RF.

In conclusion, we have shown that analysis of the metabolome in a carefully conducted clinical study can provide insights into the mechanisms underpinning physiological processes such as the response to acute CR in humans. With replication, these studies have the potential to provide valuable insights into the mechanisms underlying the effects of caloric restriction which may inform new therapeutic opportunities for weight maintenance.

Acknowledgements
We thank the volunteers who took part in the study, as well as Keith Burling and Peter Barker who performed the biochemical assays (NIHR Cambridge Biomedical Research Centre Core Biochemical Assay Laboratory). This work was supported by the Wellcome Trust (I.S.F.), the National Institute for Health Research Cambridge Biomedical Research Centre, the European Research Council, the Bernard Wolfe Health Neuroscience Fund (all to I.S.F.), the Swiss National Science Foundation (P3SMP3-155318, PZ00P3-167826, to T.H.C.), and the Uehara Memorial Foundation (to T.S.). This work was supported by the National Institute for Health Research Rare Diseases Translational Research Collaboration (NIHR RD-TRC) and the NeuroFAST consortium which is funded by the European Union's Seventh Framework Programme (FP7/2007-2013) under grant agreement no 245009. B.I. and L.G. are employees of Metabolon Inc., Durham, NC. The rest of the authors have no conflict of interest to declare.

Correspondence to Sadaf Farooqi (isf20@cam.ac.uk).

Funding support: the Wellcome Trust, the National Institute for Health Research Cambridge Biomedical Research Centre, the National Institute for Health Research Rare Diseases Translational Research Collaboration, the European Union's Seventh Framework Programme (NEUROFAST), the Bernard Wolfe Health Neuroscience Fund, the Swiss National Science Foundation and the Uehara Memorial Foundation. B.I. and L.G. are employees of Metabolon Inc., Durham, NC. Details in the Acknowledgments section.

Author contributions

I.S.F. and T.H.C. designed the study; T.H.C., E.H., J.M.K., B.I., S.K., L.G. conducted the research and acquired data; T.H.C., T.S., B.I., L.G., I.S.F. analyzed data and performed statistical analyses; T.H.C., T.S., B.I., L.G., I.S.F. wrote the paper; all authors contributed to and approved the paper.

REFERENCES

1. Friedman, J.M., *Obesity in the new millennium.* Nature, 2000. **404**(6778): p. 632-4.
2. Considine, R.V., et al., Serum immunoreactive-leptin concentrations in normal-weight and obese humans [see comments]. N Engl J Med, 1996. **334**(5): p. 292-5.
3. Maffei, M., et al., Leptin levels in human and rodent: measurement of plasma leptin and ob RNA in obese and weight-reduced subjects. Nat Med, 1995. **1**(11): p. 1155-61.
4. Rosenbaum, M., et al., Low-dose leptin reverses skeletal muscle, autonomic, and neuroendocrine adaptations to maintenance of reduced weight. J Clin Invest, 2005. **115**(12): p. 3579-86.
5. Rosenbaum, M., et al., Low dose leptin administration reverses effects of sustained weight-reduction on energy expenditure and circulating concentrations of thyroid hormones. J Clin Endocrinol Metab, 2002. **87**(5): p. 2391-4.
6. Ahima, R.S., et al., *Role of leptin in the neuroendocrine response to fasting.* Nature, 1996. **382**(6588): p. 250-2.
7. Coleman, D.L. and K.P. Hummel, *Effects of parabiosis of normal with genetically diabetic mice.* Am J Physiol, 1969. **217**(5): p. 1298-304.

8. Montague, C.T., et al., Congenital leptin deficiency is associated with severe early-onset obesity in humans. Nature, 1997. **387**(6636): p. 903-8.
9. Farooqi, I.S., et al., Effects of recombinant leptin therapy in a child with congenital leptin deficiency. N Engl J Med, 1999. **341**(12): p. 879-84.
10. Guo, L., et al., Plasma metabolomic profiles enhance precision medicine for volunteers of normal health. Proc Natl Acad Sci U S A, 2015. **112**(35): p. E4901-10.
11. Collet, T.H., et al., The Sleep/Wake Cycle is Directly Modulated by Changes in Energy Balance. Sleep, 2016.
12. Hayter, J.E. and C.J. Henry, A re-examination of basal metabolic rate predictive equations: the importance of geographic origin of subjects in sample selection. Eur J Clin Nutr, 1994. **48**(10): p. 702-7.
13. Evans, A.M., et al., Integrated, nontargeted ultrahigh performance liquid chromatography/electrospray ionization tandem mass spectrometry platform for the identification and relative quantification of the small-molecule complement of biological systems. Anal Chem, 2009. **81**(16): p. 6656-67.
14. Dehaven, C.D., et al., Organization of GC/MS and LC/MS metabolomics data into chemical libraries. J Cheminform, 2010. **2**(1): p. 9.
15. Evans, A., Bridgewater BR, Liu Q, Mitchell MW, Robison RJ, Dai H, Stewart SJ, DeHaven CD, Miller LAD, High resolution mass spectrometry improves data quantity and quality as compared to unit mass resolution mass spectrometry in high-throughput profiling metabolomics. Metabolomics, 2014.
16. Storey, J.D. and R. Tibshirani, *Statistical significance for genomewide studies.* Proc Natl Acad Sci U S A, 2003. **100**(16): p. 9440-5.
17. Fontana, L., et al., Effect of long-term calorie restriction with adequate protein and micronutrients on thyroid hormones. J Clin Endocrinol Metab, 2006. **91**(8): p. 3232-5.
18. Ravussin, E., et al., A 2-Year Randomized Controlled Trial of Human Caloric Restriction: Feasibility and Effects on Predictors of Health Span and Longevity. J Gerontol A Biol Sci Med Sci, 2015. **70**(9): p. 1097-104.
19. Lessig, J. and B. Fuchs, Plasmalogens in Biological Systems: Their Role in Oxidative Processes in Biological Membranes, their Contribution to Pathological Processes and Aging and Plasmalogen Analysis. Current Medicinal Chemistry, 2009. **16**(16): p. 2021-2041.
20. Wallner, S. and G. Schmitz, *Plasmalogens the neglected regulatory and scavenging lipid species.* Chem Phys Lipids, 2011. **164**(6): p. 573-589.
21. Hannun, Y.A. and L.M. Obeid, The ceramide-centric universe of lipid-mediated cell regulation: Stress encounters of the lipid kind. Journal of Biological Chemistry, 2002. **277**(29): p. 25847-25850.
22. Spiegel, S. and S. Milstien, *Sphingosine-1-phosphate: an enigmatic signalling lipid.* Nat Rev Mol Cell Biol, 2003. **4**(5): p. 397-407.
23. DiPatrizio, N.V. and D. Piomelli, The thrifty lipids: endocannabinoids and the neural control of energy conservation. Trends Neurosci, 2012. **35**(7): p. 403-11.
24. Mazier, W., et al., The Endocannabinoid System: Pivotal Orchestrator of Obesity and Metabolic Disease. Trends Endocrinol Metab, 2015. **26**(10): p. 524-37.
25. Orentreich, N., et al., Age changes and sex differences in serum dehydroepiandrosterone sulfate concentrations throughout adulthood. J Clin Endocrinol Metab, 1984. **59**(3): p. 551-5.
26. Cangemi, R., et al., Long-term effects of calorie restriction on serum sex-hormone concentrations in men. Aging Cell, 2010. **9**(2): p. 236-42.

27. Rubio-Aliaga, I., et al., Metabolomics of prolonged fasting in humans reveals new catabolic markers. Metabolomics, 2011. **7**(3): p. 375-387.
28. Krug, S., et al., The dynamic range of the human metabolome revealed by challenges. FASEB J, 2012. **26**(6): p. 2607-19.
29. Wanders, R.J., J. Komen, and S. Kemp, Fatty acid omega-oxidation as a rescue pathway for fatty acid oxidation disorders in humans. FEBS J, 2011. **278**(2): p. 182-94.
30. Kienesberger, P.C., et al., Identification of an insulin-regulated lysophospholipase with homology to neuropathy target esterase. Journal of Biological Chemistry, 2008. **283**(9): p. 5908-5917.
31. Cao, H.M., et al., Identification of a lipokine, a lipid hormone linking adipose tissue to systemic metabolism. Cell, 2008. **134**(6): p. 933-944.
32. Montoliu, I., et al., Serum profiling of healthy aging identifies phospho- and sphingolipid species as markers of human longevity. Aging (Albany NY), 2014. **6**(1): p. 9-25.
33. Castro-Gomez, P., et al., *Relevance of dietary glycerophospholipids and sphingolipids to human health.* Prostaglandins Leukotrienes and Essential Fatty Acids, 2015. **101**: p. 41-51.
34. Finkel, T., *The metabolic regulation of aging.* Nat Med, 2015. **21**(12): p. 1416-23.
35. Longo, V.D., et al., *Interventions to Slow Aging in Humans: Are We Ready?* Aging Cell, 2015. **14**(4): p. 497-510.
36. Fontana, L. and L. Partridge, Promoting health and longevity through diet: from model organisms to humans. Cell, 2015. **161**(1): p. 106-18.
37. Won, E.Y., et al., Gender-specific metabolomic profiling of obesity in leptin-deficient ob/ob mice by 1H NMR spectroscopy. PLoS One, 2013. **8**(10): p. e75998.
38. Mirzaei, H., J.A. Suarez, and V.D. Longo, *Protein and amino acid restriction, aging and disease: from yeast to humans.* Trends Endocrinol Metab, 2014. **25**(11): p. 558-66.
39. Rockenfeller, P., et al., *Phosphatidylethanolamine positively regulates autophagy and longevity.* Cell Death Differ, 2015. **22**(3): p. 499-508.

Figure 1. Metabolomic signature of caloric restriction. Seven hundred and seventy metabolites were measured in eight subjects at three timepoints: baseline (gray), after caloric restriction (black) and upon refeeding (white). Panel A shows the Principal Component Analysis; Principal component 1 (PC1) captured 38.5% of the variance of the dataset and discriminated well between the three study conditions, while component 2 (PC2) covered 9.4% of the variance. Changes in metabolite categories are shown in Panels B and C: Amino acids (dark orange), Peptides (light orange), Carbohydrates (red), Energy and the TCA (tricarboxylic acid) cycle (pink), Lipids (dark green), Nucleotides (light green), Cofactors and vitamins (dark blue), and Xenobiotics (light blue). Panel B shows a Volcano plot of the statistical significance as indicated by P values (y-axis) associated with fold change in each metabolite (x-axis); baseline to caloric restriction (filled circles); caloric restriction to refeeding (open circles). A large percentage of metabolites significantly increased (38%; n=295) or decreased (39%; n=300) upon caloric restriction. Panel C shows a heatmap derived from hierarchical clustering of the metabolomic data. Clustering was performed using complete linkage and Euclidean distance, where each sample is a vector with all of the metabolite values. The color scale correlates with relative metabolite abundance across the samples: the black indicates median value, red an elevation above the median, and green a decrease below the median.

Figure 2. Glycolysis and gluconeogenesis. Panel A shows statistically significant increases (red) and decreases (green) in metabolites involved in glycolysis and the TCA (tricarboxylic

acid) cycle with caloric restriction (CR, black bars) and upon refeeding (RF, white bars). Fold changes in glucose, pyruvate and TCA cycle components are shown (y-axis). Some metabolites were not measured in this assay (gray). Statistical significance is presented as follows: + for p-values between 0.001 and 0.05; * for p-values ≤0.001; ** for p-values ≤0.001 and q-values ≤0.001. Panel B shows fold changes in glucogenic amino acids and their N-acetyl-derivatives during the study. Plots show means ± SEM of the eight subjects at baseline (BL, gray), CR (black) and RF (white).

Figure 3. Fatty acid oxidation and lipolysis. Panel A shows metabolites involved in lipolysis and fatty acid oxidation that significantly increased (red) or decreased (green) with caloric restriction (CR). Some metabolites were not measured in this assay (gray). Panel B-D show fold changes in monoacylglycerols (MAG; B), medium and long-chain fatty acids (C), and acylcarnitines (CAR; D) with CR (black) and refeeding (RF, white). Lipid species are annotated using the following convention: lipid class ([number of carbon atoms]:[number of double bonds], [position of double bond(s) if known]). In addition for MAG, sn1 or sn2 indicate the esterification position in the glycerol backbone which links the acyl group. Some fatty acids are also designated by abbreviations, such as AA (arachidonic acid), DHA (docosahexaenoate), DPA (docosapentaenoate), and EPA (eicosapentaenoate). Panel E shows fold changes in ketone bodies between baseline (BL), CR and RF; means ± SEM are shown. Panel F shows fold changes with CR (black) and RF (white) in other lipid species involved in fatty acid oxidation. Statistical significance is presented as follows: + for p-values between 0.001 and 0.05; * for p-values ≤0.001; ** for p-values ≤0.001 and q-values ≤0.001.

Figure 4. Phospholipids and other lipid mediators. Fold changes in phospholipids and other lipid mediators with caloric restriction (CR, black) and refeeding (RF, white): Glycerophospholipids (Panel A), plasmalogens (B), lysophospholipids (C), sphingomyelins (D). Lipid species are abbreviated as such: LPC, lysophosphatidylcholine; LPE, lysophosphatidylethanolamine; PC, phosphatidylcholine; PE, phosphatidylethanolamine; PPC, plasmalogen phosphatidylcholine; PPE, plasmalogen phosphatidylethanolamine; SM, sphingomyelin. The acyl group(s) are specified using the following convention: [number of carbon atoms]:[number of double bonds], [position of double bond(s) if known]; or the total numbers if unknown. In addition for LPC and LPE, sn1 or sn2 indicate the esterification position in the glycerol backbone which links the acyl group. $PC(18:0/20:3)_a$ and $PC(18:0/20:3)_b$ are structurally similar but differ by the position of the double bonds. The precise structure of $PC(38:5)_a$ and $PC(38:5)_b$ could not be specified. Statistical significance is presented as follows: + for p-values between 0.001 and 0.05; * for p-values ≤0.001; ** for p-values ≤0.001 and q-values ≤0.001. Panel E shows fold changes in endocannabinoids between baseline (BL), CR and RF; means ± SEM are shown.

Figure 5. Amino acids and Steroid Hormones. Panel A shows fold changes in the branched chain amino acids (BCAA) valine, isoleucine and leucine between baseline (BL), caloric restriction (CR) and refeeding (RF); means ± SEM are shown. Steps in BCAA catabolism are shown; metabolites that significantly increased (red) or decreased (green) with CR are indicated. Some metabolites were not measured in this assay (gray). Panel B shows fold changes in a subset of steroid hormones between conditions; means ± SEM are shown.

Table 1. Changes in fasting biochemistry in caloric restriction and upon refeeding

Mean (SEM)	Baseline	Caloric restriction	Refeeding	P values for overall comparison			
				Overall	BL-CR	CR-RF	BL-RF
Caloric intake, kcal/day	2255 (53)	226 (5)	4552 (324)	<0.0001	<0.001	<0.001	<0.001
Glucose metabolism [a]							
Glucose, mmol/l	4.74 (0.12)	3.48 (0.08)	4.70 (0.11)	<0.0001	<0.001	<0.001	1.00
Insulin, pmol/l	44.6 (7.7)	14.6 (2.6)	87.6 (14.2)	<0.0001	<0.001	<0.001	<0.001
Glucagon, pg/ml	24.8 (2.7)	74.7 (11.6)	38.2 (4.2)	0.0001	<0.001	<0.001	0.01
3-OH butyrate, µmol/l	101.8 (7.8)	1763 (258)	93.7 (7.4)	<0.0001	<0.001	<0.001	1.00
Leptin, ng/ml	3.26 (0.81)	0.66 (0.19)	4.55 (1.34)	<0.0001	<0.001	<0.001	0.22
Lipid metabolism [b]							
Total cholesterol, mmol/l	4.11 (0.34)	4.30 (0.29)	3.73 (0.27)	0.0009	0.18	<0.001	0.006
Triglycerides, mmol/l	1.31 (0.11)	1.24 (0.10)	1.52 (0.14)	0.10			
Thyroid function [c]							
TSH, mU/l	1.34 (0.18)	1.14 (0.19)	2.00 (0.29)	0.006	0.20	0.001	0.04
Free T4, pmol/l	13.93 (0.35)	14.80 (0.51)	14.94 (0.47)	0.03	0.07	1.00	0.03
Free T3, pmol/l	5.02 (0.19)	3.92 (0.17)	4.65 (0.28)	0.001	<0.001	0.002	0.12
Steroids [c]							
Testosterone, nmol/l	18.51 (2.10)	17.05 (2.52)	15.27 (2.12)	0.10			
DHEAS, µg/dl	312.2 (43.8)	347.1 (39.9)	298.6 (49.7)	0.10			

Abbreviations: 3-OH butyrate, 3-hydroxybutyrate; BL, baseline; CR, caloric restriction; DHEAS, dehydroepiandrosterone sulfate; RF, refeeding; T3, tri-iodothyronine; T4, thyroxine; TSH, thyroid-stimulating hormone.

Footnotes: Data are presented as mean values and standard error of the mean (SEM). We tested the correlation of biochemistry assay concentrations with levels measured by metabolomics: the Pearson correlation ranged between $\rho = 0.87$ and $\rho = 0.95$ (for glucose, 3-OH butyrate and DHEAS), but was lower for cholesterol ($\rho = 0.70$; our metabolomics platform measures free cholesterol whereas the standard clinical assay measures total cholesterol) and free T4 ($\rho = 0.50$). [a] To convert glucose values to milligrams per deciliter, multiply by 18. To convert 3-OH butyrate values to milligrams per deciliter, divide by 96.09. Reference ranges for insulin: 0-60 pmol/l; 3-OH butyrate: 20-270 µmol/l. [b] To convert lipid values to milligrams per deciliter, multiply by 38.7 for total cholesterol and 88.5 for triglycerides. [c] Reference ranges for TSH: 0.35-5.5 mU/l; free T4: 10.0-19.8 pmol/l; free T3: 3.5-6.5 pmol/l; testosterone: 8.0-29.0 nmol/l, DHEAS: 161.2-561.6 µg/dl.

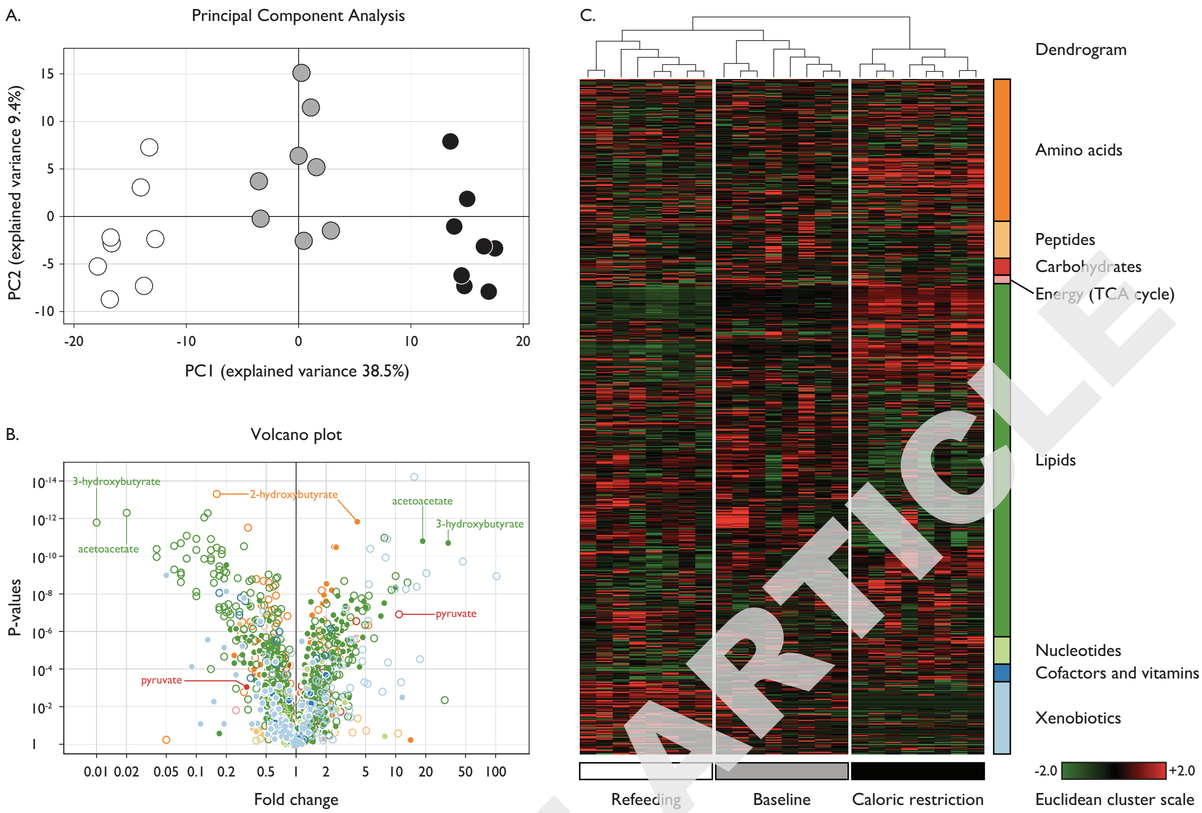
A.
Principal Component Analysis
PC2 (explained variance 9.4%)
PC1 (explained variance 38.5%)
B.
Volcano plot
3-hydroxybutyrate
2-hydroxybutyrate
acetoacetate
3-hydroxybutyrate
acetoacetate
pyruvate
pyruvate
P-values
Fold change
C.
Dendrogram
Amino acids
Peptides
Carbohydrates
Energy (TCA cycle)
Lipids
Nucleotides
Cofactors and vitamins
Xenobiotics
-2.0
+2.0
Euclidean cluster scale
Refeeding
Baseline
Caloric restriction

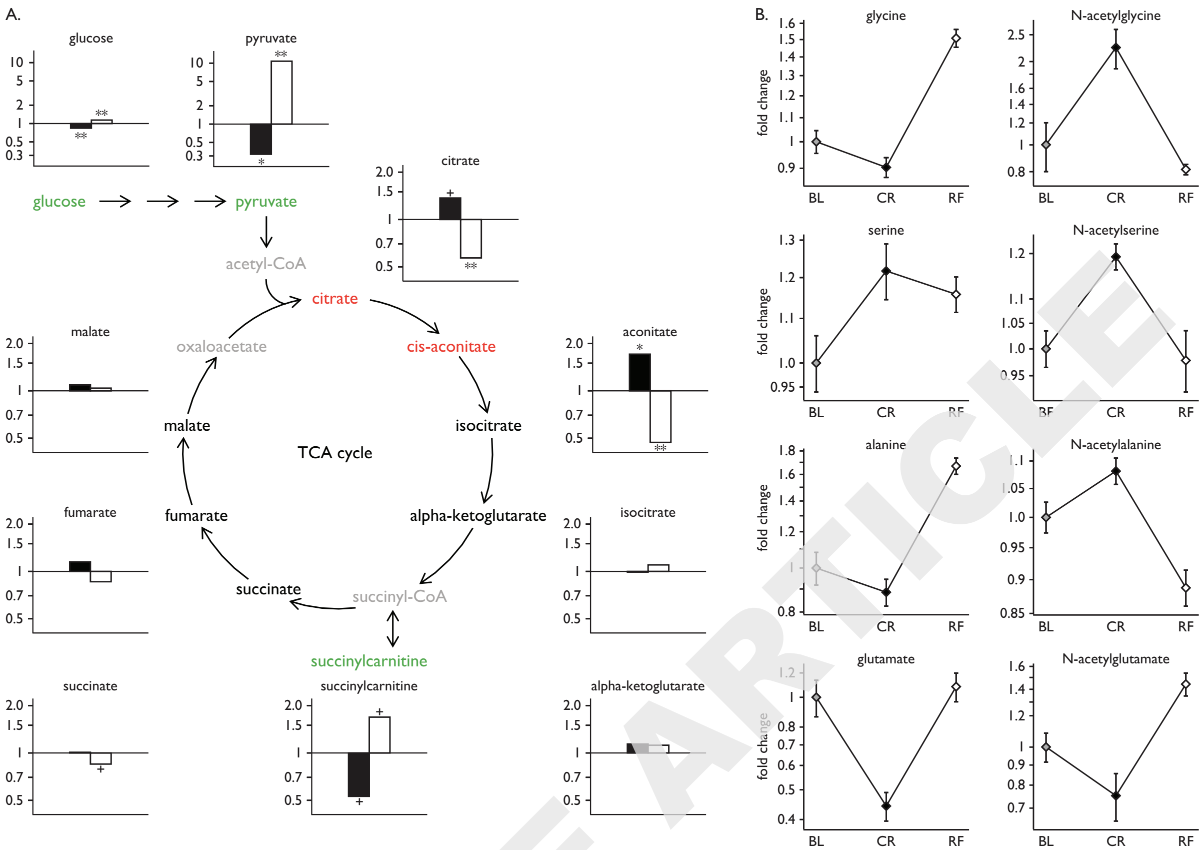
A.
glucose
pyruvate
citrate
glucose
pyruvate
acetyl-CoA
citrate
cis-aconitate
isocitrate
alpha-ketoglutarate
succinyl-CoA
succinate
fumarate
malate
oxaloacetate
TCA cycle
succinylcarnitine
malate
fumarate
succinate
succinylcarnitine
aconitate
isocitrate
alpha-ketoglutarate
B.
glycine
N-acetylglycine
serine
N-acetylserine
alanine
N-acetylalanine
glutamate
N-acetylglutamate
fold change
BL
CR
RF

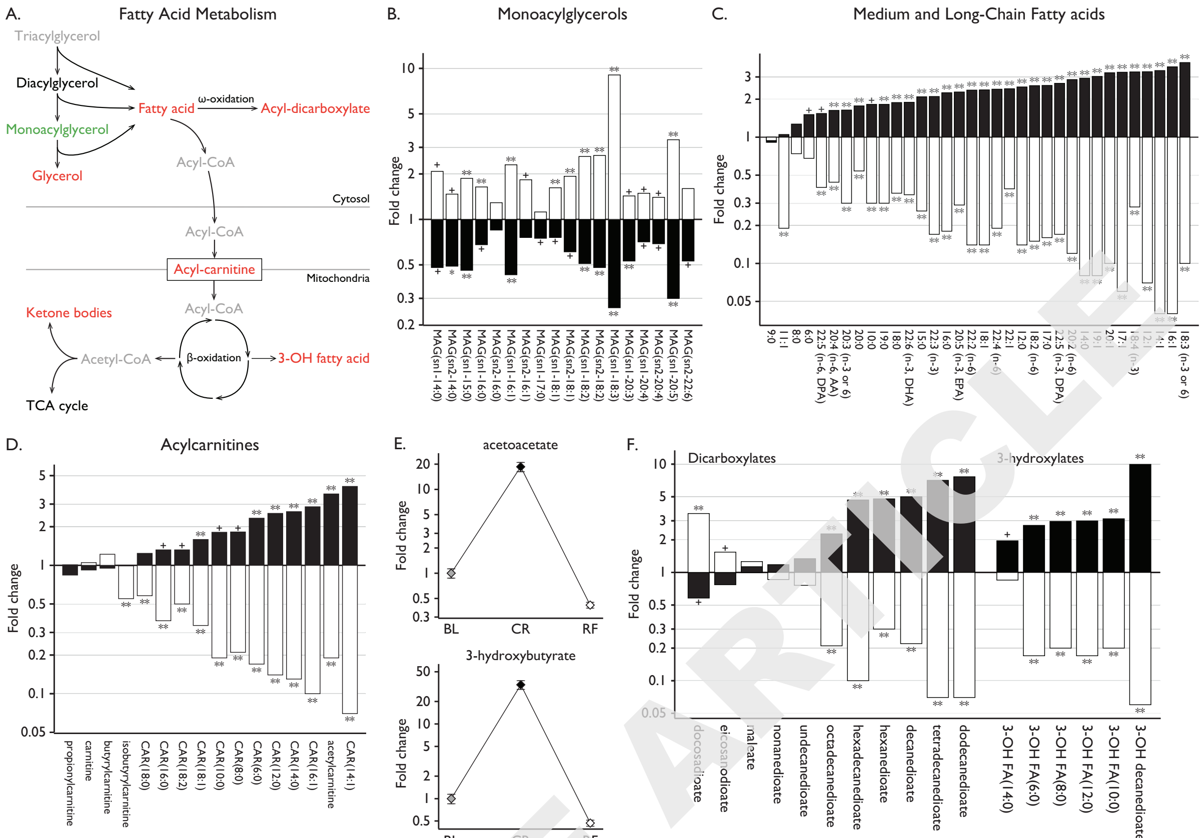
A.
Fatty Acid Metabolism
Triacylglycerol
Diacylglycerol
Fatty acid
ω-oxidation
Acyl-dicarboxylate
Monoacylglycerol
Glycerol
Acyl-CoA
Cytosol
Acyl-CoA
Acyl-carnitine
Mitochondria
Acyl-CoA
Ketone bodies
Acetyl-CoA
β-oxidation
3-OH fatty acid
TCA cycle
B.
Monoacylglycerols
Fold change
MAG(sn1-14:0)
MAG(sn2-14:0)
MAG(sn1-15:0)
MAG(sn1-16:0)
MAG(sn2-16:0)
MAG(sn1-16:1)
MAG(sn2-16:1)
MAG(sn1-17:0)
MAG(sn1-18:1)
MAG(sn2-18:1)
MAG(sn1-18:2)
MAG(sn2-18:2)
MAG(sn1-18:3)
MAG(sn1-20:3)
MAG(sn1-20:4)
MAG(sn2-20:4)
MAG(sn1-20:5)
MAG(sn2-22:6)
C.
Medium and Long-Chain Fatty acids
Fold change
D.
Acylcarnitines
Fold change
propionylcarnitine
carnitine
butyrylcarnitine
isobutyrylcarnitine
CAR(18:0)
CAR(16:0)
CAR(18:2)
CAR(18:1)
CAR(10:0)
CAR(8:0)
CAR(6:0)
CAR(12:0)
CAR(14:0)
CAR(16:1)
acetylcarnitine
CAR(14:1)
E.
acetoacetate
Fold change
BL
CR
RF
3-hydroxybutyrate
Fold change
F.
Dicarboxylates
3-hydroxylates
Fold change
docosadioate
eicosanodioate
nonanedioate
undecanedioate
octadecanedioate
hexadecanedioate
hexanedioate
decanedioate
tetradecanedioate
dodecanedioate
3-OH FA(14:0)
3-OH FA(6:0)
3-OH FA(8:0)
3-OH FA(12:0)
3-OH FA(10:0)
3-OH decanediote

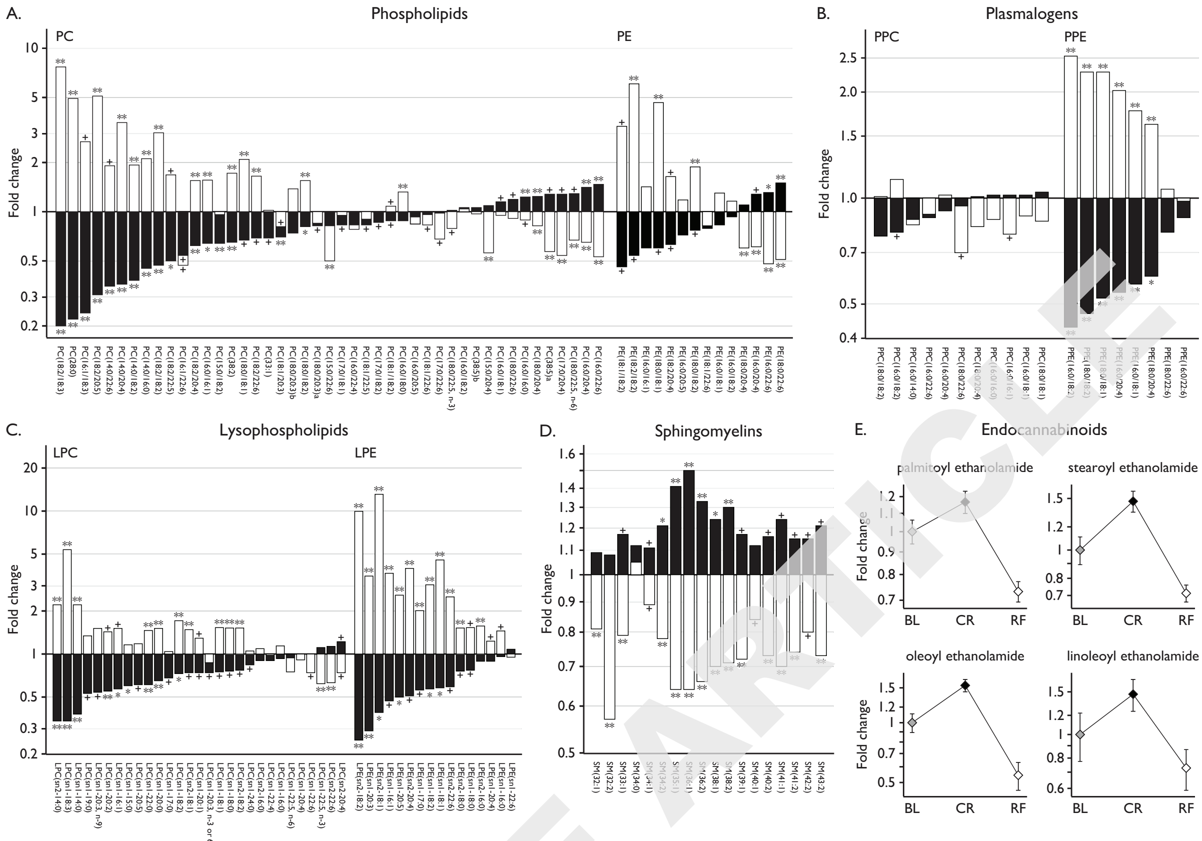
A.
Phospholipids
PC
PE
Fold change
B.
Plasmalogens
PPC
PPE
C.
Lysophospholipids
LPC
LPE
D.
Sphingomyelins
E.
Endocannabinoids
palmitoyl ethanolamide
stearoyl ethanolamide
oleoyl ethanolamide
linoleoyl ethanolamide
BL
CR
RF

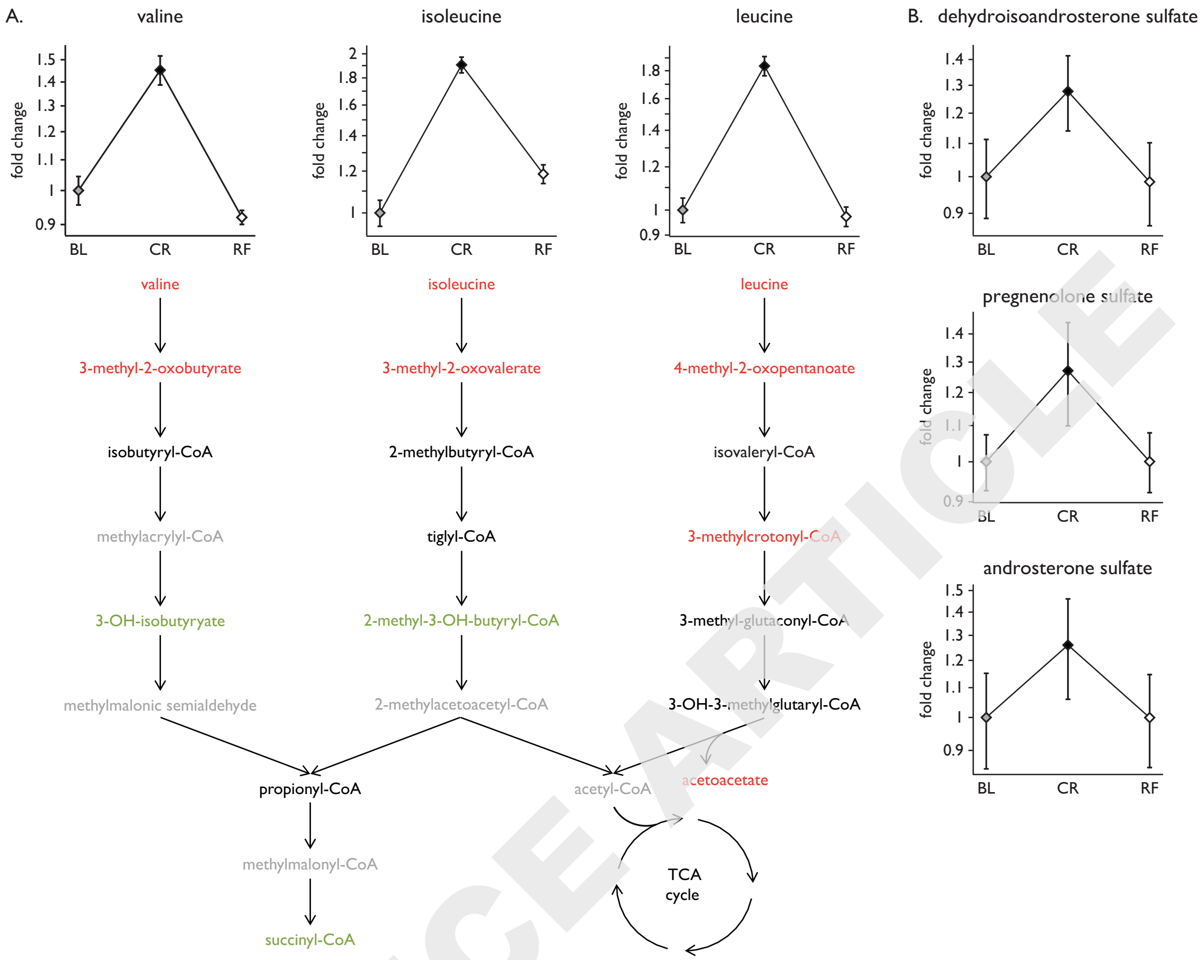
A.
valine
isoleucine
leucine
fold change
BL
CR
RF
valine
3-methyl-2-oxobutyrate
isobutyryl-CoA
methylacrylyl-CoA
3-OH-isobutyryate
methylmalonic semialdehyde
isoleucine
3-methyl-2-oxovalerate
2-methylbutyryl-CoA
tiglyl-CoA
2-methyl-3-OH-butyryl-CoA
2-methylacetoacetyl-CoA
leucine
4-methyl-2-oxopentanoate
isovaleryl-CoA
3-methylcrotonyl-CoA
3-methyl-glutaconyl-CoA
3-OH-3-methylglutaryl-CoA
acetoacetate
propionyl-CoA
acetyl-CoA
methylmalonyl-CoA
succinyl-CoA
TCA
cycle
B. dehydroisoandrosterone sulfate
pregnenolone sulfate
androsterone sulfate